35th Annual International Conference of the IEEE EMBS
Osaka, Japan, 3 - 7 July, 2013

Investigation of the photoelectrochemical effect in optoelectrodes and potential uses for implantable electrode characterization*

Abeer Khurram, *Member, IEEE* and John P. Seymour, *Member, IEEE*

***Abstract*—The combination of optical stimulation and electrical recording is commonly employed in neuroscience research. Researchers using optogenetics are familiar with the photo-induced "artifacts" that arise from illumination of an electrode array. We sought to characterize this photoelectrochemical (PEC) effect to understand the underlying mechanism seen on NeuroNexus optoelectrodes. In doing so, we discovered that the phenomenon is inversely proportional to electrode site area in the same manner as electrical impedance measurements. We have applied the PEC effect as a method of electrode evaluation and show that a PEC measurement system can be both faster and more effective than impedance at sensing defects in high-throughput biomedical device testing.**

I. Introduction

Electrical impedance spectroscopy (EIS) is widely used to characterize implantable electrodes [1–4]. In particular, impedance at 1 kHz is important for neural recording electrodes since the pulse width of an action potential is approximately 1 ms. However, there are several limitations in impedance when it comes to automated measurement of medical devices with implantable electrodes. Conventional neuromodulation devices have increasing electrode counts and thin-film MEMS-based devices may have hundreds of electrodes. A single wafer may contain 20,000 to 100,000 microelectrodes, and with a measurement time of two to twelve seconds per channel (depending on the system being used), impedance measurements limit testing throughput. Moreover, detecting defects like opens and shorts are not always decisive for reasons we explain. Automated 100% unit testing of thousands of devices on a wafer requires a fast technique that is especially sensitive to defects like opens and short-circuits.

An alternative to impedance is the photoelectrochemical (PEC) effect. The discovery of photoelectrochemistry dates to 1839, when a nineteen-year-old French scientist discovered that two platinum plates in an electrolyte generated a current upon illumination of one of the plates [5]. Since the 1960s, the field of photoelectrochemistry has been well-established and is best known for its contributions to solar energy production [6–8]. Neuroscientists utilizing optogenetic techniques [9–11] to stimulate neurons are familiar with this phenomenon as a photo-induced "artifact" [12–14]. In this study we apply the basic PEC effect, which is the generation of a voltage or current transient when light is incident on a metal/electrolyte interface, to the practical application of electrode verification.

An objective of this study is to explain how the PEC effect can be used as a faster, more reliable technique for neural electrode characterization instead of impedance. We also characterize the PEC response for various parameters, which is useful in understanding the underlying mechanism.

II. Methods

A. Device Fabrication and Assembly

Neural devices were fabricated and assembled by NeuroNexus, a subsidiary of Greatbatch, Inc. Polyimide devices were used in all experiments for consistency, which were manufactured using a polyimide upper and lower dielectric and metal electrode sites and traces. The site material was platinum or gold. Silicon devices may also be used if fabricated with precise doping levels. Otherwise, a photovoltaic effect is a common occurrence with semiconductor materials that will confound the measurement of the PEC effect.

B. Setup

Each device was mounted in separate glass dishes using UV-curable epoxy. The dish was filled with an electrolyte of 1X PBS unless otherwise stated. The 16-channel connector on the device was attached to the RA16AC headstage, which was connected to the Medusa pre-amplifier RA16PA and RX7 system (Tucker-Davis Technologies, Alachua, FL). A counter electrode wire was soldered on the headstage dip-pin connector and then connected to a gold wire placed in the electrolyte. The glass dish was attached to a 3-axis micromanipulator (Fig. 1).

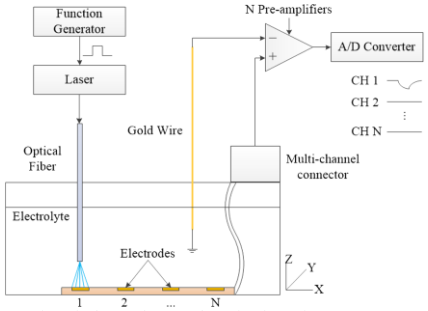

Fig. 1. Schematic of photoelectrochemical testing setup.

Impedance was recorded with PGSTAT12 (Metrohm Autolab, Utrecht, The Netherlands) at 1 kHz with a 25 mV input sine wave. The PGSTAT12 applies 256 cycles and measures the average response. Measurements were taken with a multiplexer. For PEC measurements, a patch cord was created using a 105 µm core diameter optical fiber (Thorlabs, Newton, NJ). One end of the patch cord was connected to the

*Research supported by NeuroNexus and SBIR 1R43NS073185-01.

A. Khurram is with NeuroNexus, Ann Arbor, MI 48108, USA (e-mail: akhurram@neuronexus.com).

J. P. Seymour is also with NeuroNexus, Ann Arbor, MI 48108, USA (e-mail: jseymour@neuronexus.com).

473 nm laser diode output on an MCLS1 laser diode system (Thorlabs) while the other end was secured in a ferrule. The fiber was also attached to a vertical manipulator such that the ferrule was orthogonal to the plane of the device under test. A function generator (Agilent Technologies, Santa Clara, CA) was used to drive the MCLS1 at various frequencies and duty cycles. The optical power output of the fiber was confirmed with an S140C integrating sphere photodiode power sensor (Thorlabs). The fiber was placed flush to the site unless otherwise indicated.

C. Testing Opens and Shorts

To create an open channel, a trace leading to a site was severed with a razor. The cut portion was then covered with UV-curable epoxy to isolate the site completely from the electrolyte solution. Impedance was measured in 1X PBS at 1 kHz. The PEC signal was also recorded as light was pulsed on the opened site.

To short sites on a device, two channels were physically joined together with a wire on the pre-amplifier connector. Impedance was measured in this configuration, and the PEC signal was recorded as light was pulsed on individual channels.

D. PEC Signal and Analysis

Measuring the PEC effect with a galvanostat requires a three-electrode setup. We used an Ag/AgCl reference electrode (Bioanalytical Systems, West Lafayette, IN) and a gold wire counter electrode. The electrode site on the device served as the working electrode. As shown in Fig. 2. A, a positive current peak occurs when light is turned on and rapidly decays to the baseline value. When light is turned off, an opposite current peak occurs. A MATLAB script was used to average ≥5 peaks and integrate them over time to find the charge transferred at the electrode surface. As measured with a potentiostat or high-impedance amplifier, the PEC effect results in polarization of the electrode surface when light is turned on and depolarization when the light turns off. A MATLAB script was used to calculate the peak-to-peak amplitude of the signal. The standard PEC signal was displayed as the average of 200 PEC events ± standard deviation (Fig. 2. B).

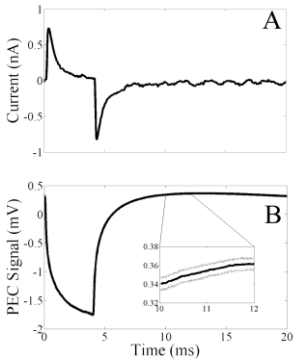

Fig. 2. Two different representations of the PEC effect. Light pulsed at 50 Hz, 20% duty. Device used for testing had 50µm diameter Au sites. A) Amperometry data collected with PGSTAT12 shows a positive peak at light turn-on and a reverse peak when light is off. Signal shown is average of 20 events. B) Voltage data collected with TDT system shows polarization of electrode at light turn-on and depolarization at light turn-off. A similar response is reported by Gan with pulsed light [15]. Inset shows the average PEC signal for 200 events ± SD.

The open-circuit voltage measured with potentiometry is often used to characterize the light conversion efficiency of solar cells [7], [15], [16]. For this reason, along with the ease of setup and ability to view the PEC signal real-time, potentiometry was used in our study.

III. RESULTS

A. PEC Effect as Function of Irradiance

The peak-to-peak amplitude of the PEC effect increases linearly with light irradiance (Fig. 3). An inflection point occurs in the PEC signal amplitude while the laser is still in LED mode at 1.5 mW/mm^2 (lasing begins around 2.4 mW/mm^2). This inflection point is defined as our lowest detection limit.

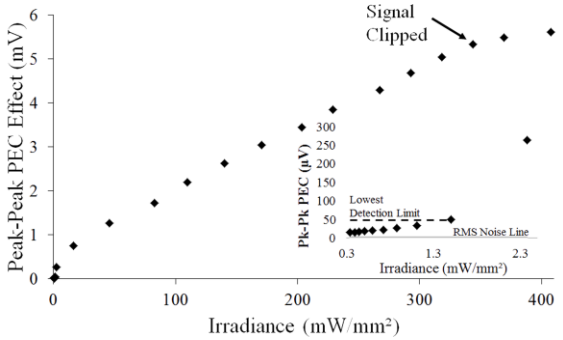

Fig. 3. PEC signal increases linearly with irradiance. Due to the upper limit on our pre-amplifier (±8 mV), the signal was clipped around 350 mW/mm². A 15 µV signal is detected even at very low irradiance of 0.3 mW/mm² (inset). RMS Noise Line is at 2.4 µV in inset. The lowest detection limit of 50 µV was determined by the inflection point around 1.5 mW/mm². Device had 50 µm diameter Au sites.

B. Sensitivity to Site Area

The inverse relationship between impedance and site area is a well-known phenomenon. To characterize PEC in a similar fashion, artifact was measured on different site sizes ranging from 0 to 600 µm diameter, which spans open-circuit to microelectrode to neuromodulation-size electrodes. Fig. 4 reveals a strong correlation between impedance and artifact for relatively large site areas whereas the pattern breaks for microelectrode areas (< 1960 µm^2).

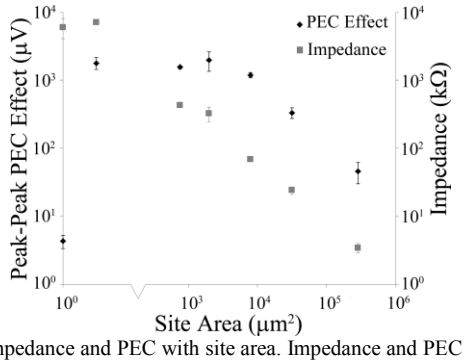

Fig. 4. Impedance and PEC with site area. Impedance and PEC are both linear in the macroscale region. While impedance maintains linearity in the microscale region, PEC reaches an inflection point and drops for an open site (defined as area = 1). Light pulsed at 50Hz, 25% duty, 1 mW power output with fiber positioned 1 mm above site. Devices tested had Pt sites.

Impedance increases as the site approaches the ~200 µm^2 range where sensitivity is poor due to capacitive loading of

the multiplexer and leads. Conversely, the PEC signal reaches an inflection point around a site diameter of 50 µm (1960 µm^2). Interestingly, there is not much difference in average peak-to-peak PEC amplitude between a 3 µm^2 area and a 750 µm^2 area. We hypothesize that this will be linear for a lower irradiance value.

C. Sensitivity to Electrolyte

In order to test the effect of chemical environment, PEC and impedance were recorded in different electrolyte solutions ranging in pH from 2 to 13 (Fig. 5. A). Impedance peaks for DI water and rapidly decreases with addition of a small amount of HCl or KOH (Sigma Aldrich, St. Louis, MO). Impedance is highly dependent on the availability of a requisite amount of ions and is not sensitive to the species present in solution. On the other hand, PEC is more sensitive to concentration, especially at low concentration of HCl. The signal morphology is different for HCl and KOH solutions, which indicates that PEC is sensitive to chemical species as well (Fig. 5. B).

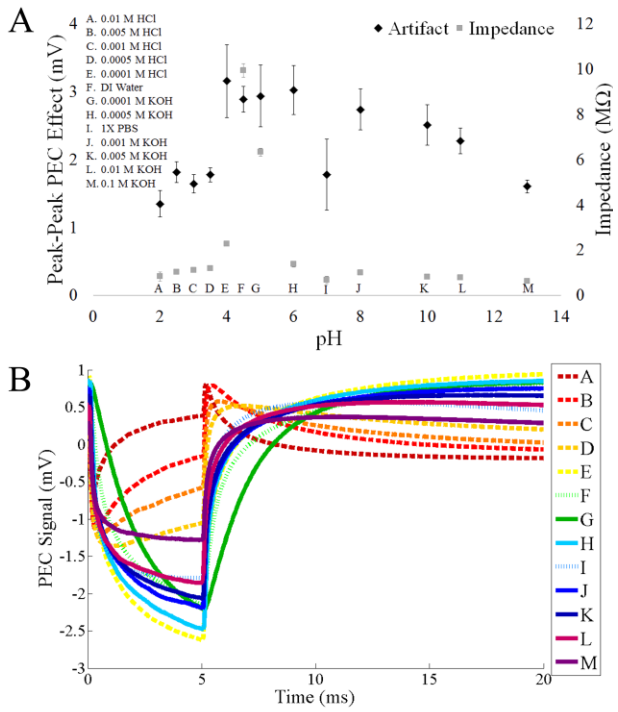

Fig. 5. Peak-to-peak signal and morphology in solutions of varying pH. Light modulated at 50 Hz, 25% duty, 1 mW output with fiber positioned at a distance of ~ 0 mm from the electrode site. Device used for testing had 50µm diameter Au sites. A) Peak-to-peak PEC amplitude and impedance for n = 3 sites. B) PEC signal morphology in various solutions on one site.

Notice the high error bars for PEC as compared to impedance. We believe the main reason for this discrepancy is that impedance measurement is fully automated but the PEC setup requires precision placement of the light source relative to the electrode. At a close distance to the site, any angle in the fiber may cause a decrease in the PEC amplitude if the site is not uniformly illuminated. Also, measuring PEC on each site requires us to manually position the fiber on the next site which introduces error in X, Y, Z positioning. We expect greater precision with an automated PEC detection system.

D. PEC Effect as Function of Frequency and Pulse Width

To understand the effect of frequency and pulse width of light, data was recorded with a potentiostat and galvanostat. Our potentiostat data show that the morphology changes and the peak-to-peak amplitude decreases for increasing frequency (Fig. 6. A). For a particular frequency, increasing pulse width causes the baseline to shift to more positive polarity while the peak-to-peak value remains relatively stable. Our galvanostat data agree with this and show that for varying pulse width, there is not much difference in the charge transferred (Fig. 6. B & C). The resulting current is highly dependent on the change of state of the light instead of the duration of light. For neuroscientists using optoelectrodes, these results show that shorter pulse widths can significantly reduce the PEC effect amplitude.

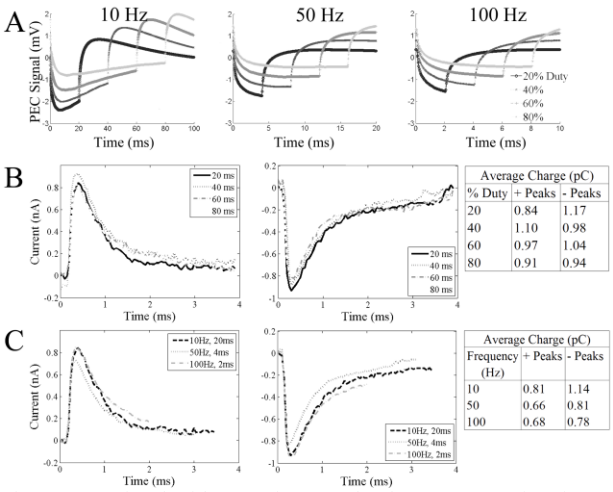

Fig. 6. PEC signal with potentiostat and galvanostat as a function of frequency and pulse width. Device used for testing had 50µm diameter Au sites. A) PEC signal morphology and peak-peak amplitude change with increasing frequency. B) Amperometry data for varying pulse width at 10 Hz. C) Amperometry data for varying frequency at 20% duty cycle. While charge values calculated for B and C seem to change little with duty cycle and frequency, further testing is required to determine statistical significance.

E. Detecting Opens and Shorts

An important benefit of a PEC measurement system is that it is more decisive in determining opens and shorts as compared to impedance. Open-circuit failures appear as no PEC signal and have high RMS noise. Fig. 7 illustrates the difference in PEC signal for an open site and a site area of ~3um^2.

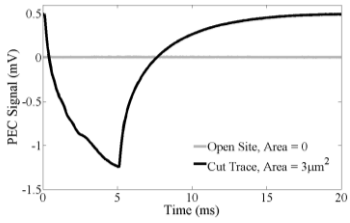

Fig. 7. No PEC effect is detected on an open site whereas a large PEC signal is detected even for a 3µm^2 area. This 3µm^2 area was created by cutting a polyimide device and exposing the trace leading to the site. Light was pulsed at 50 Hz, 25% duty, with 2 mW power output at a distance of 1 mm from the site. In comparison, the difference in impedance between an open and a 3µm^2 area is not as decisive (See Fig. 4).

Regarding short-circuit failures, the most convenient and cost-effective method to measure shorts on an impedance system is to measure impedance on all channels sequentially and then flag any two or more electrodes having a value equal in magnitude and below the average. This lacks decisiveness when there are only 2 shorts (most common) and the site-to-site variance is high. Alternatively, a custom PEC measurement system would employ low-cost multi-channel instrumentation amplifiers for simultaneous measurement while illuminating one electrode site. This accurately identifies shorts (Fig. 8) not because the phenomenon is more sensitive, but because the electronics allow for simultaneous measurements. In an automated procedure, PEC would allow for detection of all shorted sites on a device within milliseconds whereas impedance may take several seconds.

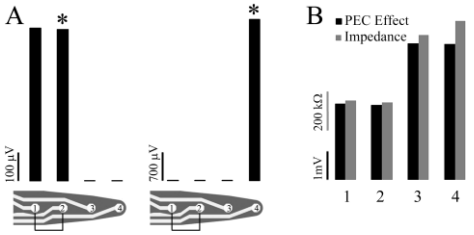

Fig. 8. Detecting shorts with PEC and impedance. A) Asterisk indicates the illuminated site. Sites 1 and 2 were shorted. When light shines on a shorted site, all corresponding shorts display a PEC signal of equal magnitude. B) Impedance and PEC provide similar information about shorts. The benefit of PEC lies in ease of simultaneous measurements.

The benefits of a PEC system can immediately be seen from the equivalent circuit (Fig. 9). When testing the impedance of microelectrodes, the measurement is loaded by the parasitic capacitance of the leads (from the various connectors and PCBs) and may be comparable to the electrode component of the circuit. There are multiple paths for the signal to return to the detector, which may lead to an open being difficult to discern from a microelectrode (especially for highly smooth surfaces and materials such as gold). Conversely, PEC creates a transient directly at the electrode, which cannot be detected if there is an open-circuit.

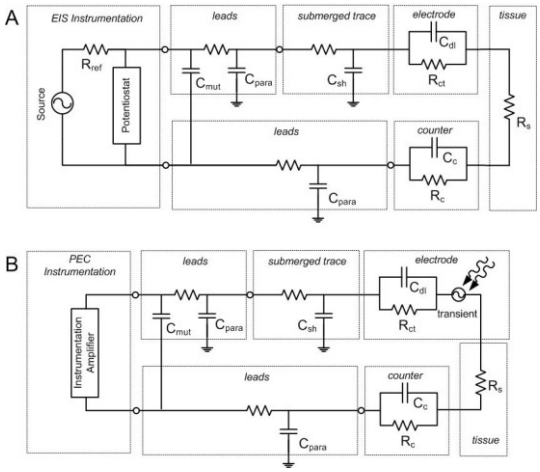

Fig. 9. Equivalent circuit for impedance and PEC. Notice that as the electrode size approaches zero, the EIS instrumentation will be dominated by the lead capacitance. PEC instrumentation accurately and easily detects open circuits. Component labels described in text.

IV. Conclusion

The photoelectrochemical effect on microelectrodes creates an unintended artifact signal during optogenetic experiments, which we have characterized in this study and will further characterize in future work. We have also found the effect creates a reliable signal that is comparable to electrical impedance spectroscopy and with a few considerable advantages. The PEC measurement we describe here provides faster, more reliable open-circuit and short-circuit detection for biomedical electrode testing. Impedance spectroscopy is still preferable for precise surface characterization based on our results.

References

[1] J. C. Williams, R. L. Rennaker, and D. R. Kipke, "Long-term neural recording characteristics of wire microelectrode arrays implanted in cerebral cortex," *Brain Res Brain Res Protoc*, vol. 4, no. 3, pp. 303–313, 1999.

[2] S. F. Cogan, "Neural stimulation and recording electrodes," *Annu Rev Biomed Eng*, vol. 10, pp. 275–309, 2008.

[3] S. L. BeMent, D. J. Anderson, K. D. Wise, K. L. Drake, K. Najafi, and L. Xue, "Silicon microelectrode impedance, geometry, and neural cell recording ability," 1985, pp. 159–162.

[4] T. J. Blanche, M. A. Spacek, J. F. Hetke, and N. V Swindale, "Polytrodes: high-density silicon electrode arrays for large-scale multiunit recording," *J Neurophysiol*, vol. 93, no. 5, pp. 2987–3000, 2005.

[5] A. E. Becquerel, "On electric effects under the influence of solar radiation," *CR Acad. Sci*, vol. 9, pp. 711–714, 1839.

[6] K. Honda, "Dawn of the evolution of photoelectrochemistry," *Journal of Photochemistry and Photobiology A: Chemistry*, vol. 166, no. 1, pp. 63–68, 2004.

[7] M. Gratzel, "Photoelectrochemical cells," *Nature*, vol. 414, no. November, 2001.

[8] S. Licht and D. Peramunage, "Efficient photoelectrochemical solar cells from electrolyte modification," *Nature*, vol. 345, no. 6273, pp. 330–333, May 1990.

[9] E. S. Boyden, F. Zhang, E. Bamberg, G. Nagel, and K. Deisseroth, "Millisecond-timescale, genetically targeted optical control of neural activity," *Nat Neurosci*, vol. 8, no. 9, pp. 1263–1268, 2005.

[10] K. Deisseroth, G. Feng, A. K. Majewska, G. Miesenbock, A. Ting, and M. J. Schnitzer, "Next-generation optical technologies for illuminating genetically targeted brain circuits," *J Neurosci*, vol. 26, no. 41, pp. 10380–10386, 2006.

[11] J. W. and F. W. and D. A. B. and J. Z. and I. O. and R. D. B. and A. V. N. and R. van W. and I. D. and K. Deisseroth, "Integrated device for combined optical neuromodulation and electrical recording for chronic in vivo applications," *Journal of Neural Engineering*, vol. 9, no. 1, p. 16001, 2012.

[12] X. Han, X. Qian, P. Stern, A. S. Chuong, and E. S. Boyden, "Informational lesions: optical perturbation of spike timing and neural synchrony via microbial opsin gene fusions," *Front Mol Neurosci*, vol. 2, p. 12, 2009.

[13] S. Royer, B. V Zemelman, M. Barbic, A. Losonczy, G. Buzsáki, and J. C. Magee, "Multi-array silicon probes with integrated optical fibers: light-assisted perturbation and recording of local neural circuits in the behaving animal.," *The European journal of neuroscience*, vol. 31, no. 12, pp. 2279–91, Jun. 2010.

[14] J. A. Cardin, M. Carlén, K. Meletis, U. Knoblich, F. Zhang, K. Deisseroth, L.-H. Tsai, and C. I. Moore, "Targeted optogenetic stimulation and recording of neurons in vivo using cell-type-specific expression of Channelrhodopsin-2.," *Nature protocols*, vol. 5, no. 2, pp. 247–54, Feb. 2010.

[15] Y. X. Gan, B. J. Gan, E. Clark, L. Su, and L. Zhang, "Converting environmentally hazardous materials into clean energy using a novel nanostructured photoelectrochemical fuel cell," vol. 47, pp. 2380–2388, 2012.

[16] K. Ren, Y. X. Gan, E. Nikolaidis, S. Al Sofyani, and L. Zhang, "Electrolyte Concentration Effect of a Photoelectrochemical Cell Consisting of TiO 2 Nanotube Anode," vol. 2013, 2013.